


SEPTEMBER 02 2016

## Azimuth-elevation direction finding using one four-component acoustic vector-sensor spread spatially as a parallelogram array **FREE**

Yang Song; Kainam Thomas Wong 



*Proc. Mtgs. Acoust.* 26, 055002 (2016)

<https://doi.org/10.1121/2.0000238>



### Articles You May Be Interested In

Directional pointing error in "spatial matched filter" beamforming at a tri-Axial velocity-sensor with non-orthogonal axes

*Proc. Mtgs. Acoust.* (January 2019)

Azimuth-elevation direction finding, using one four-component acoustic vector-sensor spread spatially along a straight line

*Proc. Mtgs. Acoust.* (June 2015)

Near-field/far-field array manifold of an acoustic vector-sensor near a reflecting boundary

*J. Acoust. Soc. Am.* (June 2016)



**ASA**

Advance your science and career as a member of the  
**Acoustical Society of America**

[LEARN MORE](#)



## 171st Meeting of the Acoustical Society of America

Salt Lake City, Utah  
23-27 May 2016

### Signal Processing in Acoustics: Paper 2aSP8

# Azimuth-elevation direction finding using one four-component acoustic vector-sensor spread spatially as a parallelogram array

**Yang Song**

*Nanyang Technological University, School of Electrical and Electronic Engineering, Singapore;*  
*yang.song@connect.polyu.hk*

**Kainam Thomas Wong**

*Hong Kong Polytechnic University, Department of Electronic and Information Engineering, Hong Kong;*  
*ktwong@ieee.org*

An acoustic vector-sensor (also called a “vector hydrophone”) consists of three uni-axial velocity-sensors (which are oriented perpendicularly with respect to each other) and one pressure-sensor. Song and Wong (*Journal of the Acoustical Society of America*, vol. 133, no. 4, pp. 1987-1995, April 2013) has advanced direction-finding formulas that allow these four component-sensors to be spaced apart in three-dimensional space, in order to extend the overall spatial aperture spanned by them, while improving the accuracy in the azimuth-elevation angle-of-arrival estimation of an acoustic emitter impinging from the far field. Whereas Song and Wong advances estimation formulas for any general arbitrary placement of the four component-sensors, this paper will focus on a special spatial geometry -- where the four component-sensors occupy the four corners of a parallelogram in three-dimensional space – thereby simplifying the earlier formulas in Song and Wong.



# 1 Introduction

There exists a sizeable literature on the use of the four-component acoustic vector sensor (a.k.a. a vector hydrophone in underwater applications) to estimate the azimuth-elevation directions-of-arrival of incident sources. Of this literature, surveys are available in [4, 6, 7].

A four-component acoustic vector sensor consists of a pressure sensor along with three identical but perpendicular uni-axial *velocity* sensors, which are often idealized as collocated. While the pressure-sensor samples the acoustic wavefield of pressure, the three uni-axial velocity-sensors corporately sample the acoustic wavefield of the particle velocity vector, which corresponds to the gradient vector of the pressure field. This gradient vector equals the negative of the incident wavefield's propagation direction, hence very useful for the estimation of an acoustic source's azimuth-elevation direction-of-arrival. More precisely, a four-component acoustic *vector*-sensor (located at the origin of the three-dimensional Cartesian coordinates) has this  $4 \times 1$  array manifold [1, 3, 5], as response to a unit-power wavefield that impinges from the far field and that has traveled through an homogeneous isotropic medium,

$$\mathbf{a}(\theta, \phi) := \begin{bmatrix} u(\theta, \phi) \\ v(\theta, \phi) \\ w(\theta) \\ 1 \end{bmatrix} := \begin{bmatrix} \sin(\theta) \cos(\phi) \\ \sin(\theta) \sin(\phi) \\ \cos(\theta) \\ 1 \end{bmatrix}, \quad (1)$$

where  $\theta \in [0, \pi]$  symbolizes the elevation-angle measured from the positive  $z$ -axis,  $\phi \in [0, 2\pi)$  denotes the azimuth-angle measured from the positive  $x$ -axis,  $u(\theta, \phi)$  denotes the Cartesian direction-cosine along the  $x$ -axis,  $v(\theta, \phi)$  represents the Cartesian direction-cosine along the  $y$ -axis, and  $w(\theta)$  refers to the Cartesian direction-cosine along the  $z$ -axis. The first, second, and third components in  $\mathbf{a}(\theta, \phi)$  correspond to the uni-axial velocity-sensors aligned along the  $x$ -axis, the  $y$ -axis, and the  $z$ -axis, respectively. These components together always produce a Frobenius norm,  $\sqrt{[u(\psi, \phi)]^2 + [v(\psi, \phi)]^2 + [w(\psi)]^2} = 1 = [\mathbf{a}(\theta, \phi)]_4$ ,  $\forall \theta, \phi$ , with  $[\cdot]_\ell$  symbolizing the  $\ell$ th element of the vector inside the square brackets.

One flaw of this acoustic vector-sensor is the zero size of its array aperture, because of the spatial collocation of all its component-sensors. This small aperture limits the obtainable accuracy for direction finding. This spatial aperture could be readily enlarged, by locating the four component-sensors at different locations. However, that would lead to spatial phase factors among these component-sensors' data, invalidating the array-manifold of (1) and invalidating the straightforward direction finding mentioned above.

This trade-off is partly resolved in [8], which shows how these four component-sensors may be spread arbitrarily over the three-dimensional space (in order to sample the impinging wavefield at *diverse* locations), while not just achieving direction finding, but to do so with increased accuracy.<sup>1</sup> This paper will focus on one specific array grid for the spreading out of these four component-sensors – the four corners of a parallelogram, while allowing the four component-sensors to be placed one at each corner in any permutation.<sup>2</sup>

<sup>1</sup>If the pressure-sensor is absent, such that the acoustic vector-sensor degenerates to a tri-axial velocity-sensor, please see [11]. If the spatially spread configuration uses only a *bi*-axial velocity-sensor, please see [10]. If the spatially spread configuration uses a *uni*-axial velocity-sensor and a pressure-sensor, please see [11].

<sup>2</sup>For another special case where the four component-sensors lie on a straight line in any permutation, please refer to [12].

## 2 Closed-Form Estimation Formulas for the Arrival Angles : Two parallel lines

Here, both lines must be parallel to one of the three Cartesian axis, but could be unequal in length, with arbitrary terminal points. For example, Figure 1 places  $S_x$  and  $S_y$  on a line parallel to  $z$ -axis, and places  $S_p$  and  $S_z$  on another line also parallel to  $z$ -axis. The coordinates of  $S_x$  and  $S_p$  are, respectively,  $(x_x, y_x, z_x)$  and  $(x_p, y_p, z_p)$ . Other spatial permutations of the four components could also do. However, the rest of this paper will focus on the particular configuration of 1, as an illustrative example. Other configurations may be analyzed analogously.

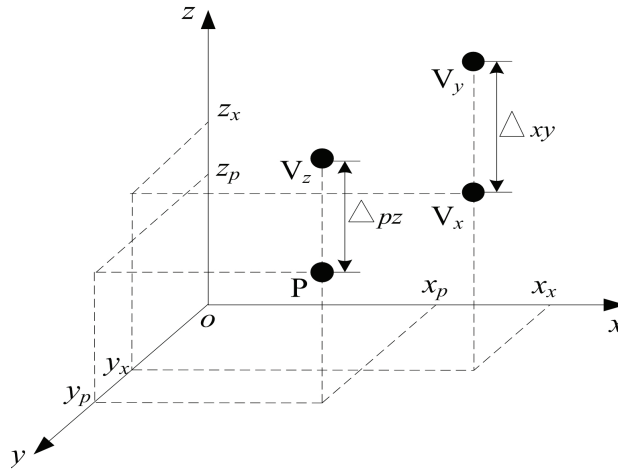


Figure 1: One configuration of an acoustic vector-sensor with its four components spatially distributed at the four corners of a parallelogram.

Using subspace-based algorithms for parameter estimation, the data-correlation matrix is eigen-decomposed to estimate each impinging source's steering vector  $\hat{\mathbf{a}} \approx c\mathbf{a}$ , to within an unknown complex number  $c$ . The approximation would be equality if there were no noise or if there were an infinite number of time-samples. That is, a subspace-based algorithm would give

$$\begin{bmatrix} p_x \\ p_y \\ p_z \\ p_p \end{bmatrix} \approx c \cdot \begin{bmatrix} u e^{j\frac{2\pi}{\lambda}(x_x u + y_x v + z_x w)} \\ v e^{j\frac{2\pi}{\lambda}[x_x u + y_x v + (z_x + \Delta_{xy})w]} \\ w e^{j\frac{2\pi}{\lambda}[x_p u + y_p v + (z_p + \Delta_{pz})w]} \\ e^{j\frac{2\pi}{\lambda}(x_p u + y_p v + z_p w)} \end{bmatrix}, \quad (2)$$

which leads to

$$\frac{p_y}{p_x} \approx \tan(\phi) e^{j\frac{2\pi}{\lambda} \Delta_{xy} w} \quad (3)$$

$$\frac{p_z}{p_p} \approx \cos(\theta) e^{j\frac{2\pi}{\lambda} \Delta_{pz} w}. \quad (4)$$

From (4), two complementary estimators of  $w$  may be devised:

{i} Note that a one-to-many relationship exists between  $e^{j2\pi \frac{\Delta_{pz}}{\lambda} w}$  and  $u \in [-1, 1]$ , despite any

extended aperture with  $\frac{\Delta_{pz}}{\lambda} > \frac{1}{2}$ . Therefore,

$$\hat{w}_{\text{phs}} = \frac{1}{2\pi} \frac{\lambda}{\Delta_{pz}} \angle \frac{p_z}{p_p} = m \frac{\lambda}{\Delta_{pz}} + w \quad (5)$$

allows the estimation of  $w$ , but ambiguously so, to within an unknown integer multiple ( $m \times$ ) of the frequency-dependent term of  $\pm \frac{\lambda}{\Delta_{pz}}$ , where  $m$  is an integer to be determined.

{ii} The frequency-independent

$$\hat{w}_{\text{mag}} = \left| \frac{p_z}{p_p} \right| = \pm w \quad (6)$$

allows the estimation of  $w$ , but also only ambiguously, now to within a  $\pm$  sign.

These two estimates,  $\hat{w}_{\text{phs}}$  and  $\hat{w}_{\text{mag}}$ , are ambiguous in different ways, but can disambiguate each other, as follows:

{a} If  $\hat{w}_{\text{mag}} = w$ , the cyclic ambiguity may be resolved by

$$\hat{m}_w^+ := \arg \min_m \left\{ \underbrace{\left( m \frac{\lambda}{\Delta_{pz}} + \overbrace{\frac{1}{2\pi} \frac{\lambda}{\Delta_{pz}} \angle \frac{p_z}{p_p}}^{=\hat{w}_{\text{phs}}} \right)}_{\stackrel{\text{def}}{=} \epsilon_w^+(m)} - \overbrace{\left| \frac{p_z}{p_p} \right|}^{=\hat{w}_{\text{mag}}} \right\}.$$

{b} If  $\hat{w}_{\text{mag}} = -w$ , the cyclic ambiguity may then be resolved by

$$\hat{m}_w^- := \arg \min_m \left\{ \underbrace{\left( m \frac{\lambda}{\Delta_{pz}} + \overbrace{\frac{1}{2\pi} \frac{\lambda}{\Delta_{pz}} \angle \frac{-p_z}{p_p}}^{=\hat{w}_{\text{phs}}} \right)}_{\stackrel{\text{def}}{=} \epsilon_w^-(m)} - \overbrace{\left| \frac{p_z}{p_p} \right|}^{=\hat{w}_{\text{mag}}} \right\}.$$

{c} To choose between  $\hat{w}_{\text{mag}} = w$  versus  $\hat{w}_{\text{mag}} = -w$ : Pick  $\hat{w}_{\text{mag}} = w$ , if  $\epsilon_w^+(\hat{m}_w^+) < \epsilon_w^-(\hat{m}_w^-)$ . Pick  $\hat{w}_{\text{mag}} = -w$ , if  $\epsilon_w^+(\hat{m}_w^+) \geq \epsilon_w^-(\hat{m}_w^-)$ .

{d} Therefore,  $w$  is now unambiguously estimated as

$$\hat{w} = \begin{cases} \left( \hat{m}_w^+ + \frac{1}{2\pi} \angle \frac{p_z}{p_p} \right) \frac{\lambda}{\Delta_{pz}}, & \text{if } \epsilon_w^+(\hat{m}_w^+) < \epsilon_w^-(\hat{m}_w^-). \\ \left( \hat{m}_w^- - \frac{1}{2\pi} \angle \frac{p_z}{p_p} \right) \frac{\lambda}{\Delta_{pz}}, & \text{if } \epsilon_w^+(\hat{m}_w^+) \geq \epsilon_w^-(\hat{m}_w^-). \end{cases}$$

Lastly, substitute  $\hat{w}$  into (3)-(4), the angle-of-arrival estimates are obtained as

$$\hat{\theta} = \arccos \hat{w}, \quad (7)$$

$$\hat{\phi} = \arctan \left( \frac{p_y}{p_x} e^{-j \frac{2\pi}{\lambda} \Delta_{pz} w} \right). \quad (8)$$

These arrival-angle estimates enjoy a support-region spanning over the hemispherical space of  $\theta \in [0, \pi)$  and  $\phi \in (0, \pi]$  (or  $\phi \in (-\pi, 0]$ ).

The above has shown how to achieve direction finding *unambiguously*, despite the four component-sensors' non-collocation and despite their sparse spacings.

### 3 Cramér-Rao Bound For Direction-Finding Using the Proposed Spatially Extended Acoustic Vector-Sensor

By spatially spreading the four components of the vector sensor into a parallelogram, the spatial aperture is extended from the collocated case's point-like geometry. This extended aperture costs no additional component-sensors but can improve direction finding accuracy. This possible improvement is shown through the Cramér-Rao lower bound, which floors the estimation error variance obtainable for any unbiased estimator.

Express the collected data as

$$\begin{aligned} \mathbf{z} &= [\tilde{\mathbf{z}}(T_s)^T, \dots, \tilde{\mathbf{z}}(MT_s)^T]^T \\ &= \underbrace{\mathbf{s} \otimes \mathbf{a}}_{\stackrel{\text{def}}{=} \boldsymbol{\mu}} + \underbrace{[\tilde{\mathbf{n}}(T_s)^T, \dots, \tilde{\mathbf{n}}(MT_s)^T]^T}_{\stackrel{\text{def}}{=} \mathbf{n}}, \end{aligned} \quad (9)$$

with

$$\tilde{\mathbf{z}}(mT_s) = \mathbf{a}s(mT_s) + \tilde{\mathbf{n}}(mT_s), \quad (10)$$

and

$$\begin{aligned} \mathbf{s} &\stackrel{\text{def}}{=} [s(T_s), \dots, s(MT_s)]^T \\ \mathbf{z} &\sim \mathcal{N}(\boldsymbol{\mu}, \boldsymbol{\Gamma}), \end{aligned} \quad (11)$$

where  $s(mT_s) \stackrel{\text{def}}{=} e^{j(mT_s + \epsilon)}$  symbolizes the received signal at the time instant of  $mT_s$ ,  $\tilde{\mathbf{n}}(mT_s)$  denotes the  $4 \times 1$  zero-mean additive white noise vector at the time of  $mT_s$ , and  $\boldsymbol{\Gamma}$  represents the covariance of additive noise, i.e.  $\boldsymbol{\Gamma} = E[\mathbf{nn}^H]$ , where  $H$  denotes the Hermitian transposition. For simplicity, further assume that the source's frequency  $\omega$  and initial phase  $\epsilon$  are prior known constants.

Group the to-be-estimated parameters in the measurement model into a vector,

$$\boldsymbol{\psi} = [\theta, \phi, \sigma^2]^T \quad (12)$$

where  $\sigma^2$  denotes the noise power.

If  $\mathbf{z}$  is Gaussian, the  $2 \times 2$  Fisher Information Matrix (FIM)  $\mathbf{J}$  would have its  $(i, j)$ th entry equal to (equation (8.34) in [2])

$$J_{i,j} = 2\Re \left[ \left( \frac{\partial \boldsymbol{\mu}}{\partial [\boldsymbol{\psi}]_i} \right)^H \boldsymbol{\Gamma}^{-1} \left( \frac{\partial \boldsymbol{\mu}}{\partial [\boldsymbol{\psi}]_j} \right) \right] + \text{Tr} \left[ \boldsymbol{\Gamma}^{-1} \frac{\partial \boldsymbol{\Gamma}}{\partial [\boldsymbol{\psi}]_i} \boldsymbol{\Gamma}^{-1} \frac{\partial \boldsymbol{\Gamma}}{\partial [\boldsymbol{\psi}]_j} \right]. \quad (13)$$

Consider the specific configuration in Figure 2 to spatially distribute the acoustic vector-sensor,

which is a special case of the more general configuration in Figure 1. Here in Figure 2, the four

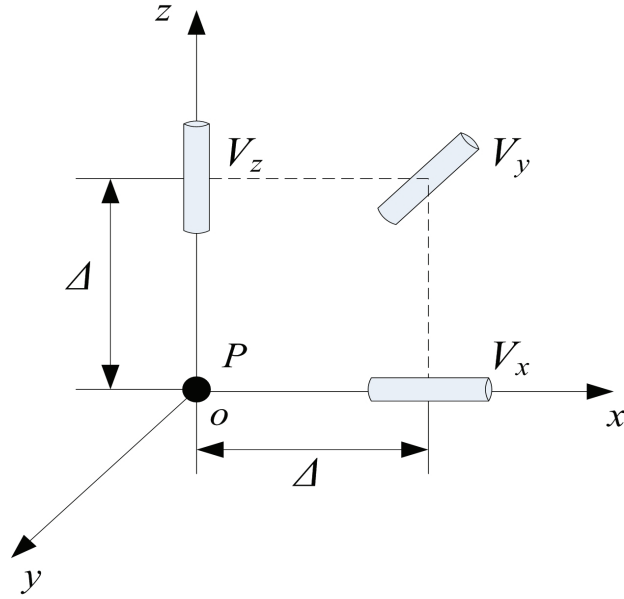


Figure 2: A special case of 1, used in the Cramér-Rao bound graphs in Figure 3.

components lies on the  $x$ - $z$  Cartesian plane, with the pressure-sensor at origin, at identical inter-component spacings of  $\Delta$ .

For this special array grid, straight-forward manipulations of the earlier stated equations would give the four scalars,

$$\begin{aligned}
 J_{1,1} &= \frac{2M}{\sigma^2} \left\{ \left( \pi \frac{\Delta}{\lambda} \right)^2 \left[ 2 \cos^4(\phi) \sin^2(\theta) \cos^2(\theta) - \frac{1}{4} (-2 \sin(2\phi) + \sin(4\phi) + 2 \cos(2\phi) - 6) \sin^2(2\theta) \right] + \right\} \\
 J_{2,2} &= \frac{2M}{\sigma^2} \sin^2(\theta) \left\{ 2 \left( \pi \frac{\Delta}{\lambda} \right)^2 (-2 \sin(2\phi) + \cos(2\phi) + 3) \sin^2(\theta) \sin^2(\phi) + 1 \right\} \\
 J_{1,2} = J_{2,1} &= -\frac{2M}{\sigma^2} \left( \pi \frac{\Delta}{\lambda} \right)^2 \sin(\phi) \sin^3(\theta) \cos(\theta) [2 \sin(\phi) - 2 \sin(3\phi) + 3 \cos(\phi) + \cos(3\phi)],
 \end{aligned}$$

explicitly in terms of the model parameters.

Then, the Cramér-Rao bounds may be obtained:

$$\begin{aligned}
 &\text{CRB}(\theta) \\
 &= [\mathbf{J}^{-1}]_{(1,1)} \\
 &= \frac{\sigma^2}{2M} \frac{1 + 2 \left( \pi \frac{\Delta}{\lambda} \right)^2 (3 + \cos(2\phi) - 2 \sin(2\phi)) \sin^2(\theta) \sin^2(\phi)}{- \left( \frac{\Delta}{\lambda} \right)^4 \pi^4 \cos^2(\theta) \sin^2(\phi) (3 \cos(\phi) + \cos(3\phi) + 2 \sin(\phi) - 2 \sin(3\phi))^2 \sin^4(\theta)} \\
 &\quad + \frac{1}{4} \left( \cos^2(\phi) + \sin^2(\phi) \left( 1 + 2 \left( \frac{\Delta}{\lambda} \right)^2 \pi^2 (3 + \cos(2\phi) - 2 \sin(2\phi)) \sin^2(\theta) \right) \right) \\
 &\quad \left( 4 + 16 \left( \frac{\Delta}{\lambda} \right)^2 \pi^2 \cos(\phi)^4 \sin^2(\theta) \cos^2(\theta) - \left( \frac{\Delta}{\lambda} \right)^2 \pi^2 (-6 + 2 \cos(2\phi) - 2 \sin(2\phi) + \sin(4\phi)) \sin^2(2\theta) \right),
 \end{aligned} \tag{14}$$

$$\begin{aligned}
& \text{CRB}(\phi) \\
&= [\mathbf{J}^{-1}]_{(2,2)} \\
&= \frac{\sigma^2 \csc^2(\theta) \left( 1 + 4 \left( \frac{\Delta}{\lambda} \right)^2 \cos(\phi)^4 \sin^2(\theta) \cos^2(\theta) - \frac{1}{4} \left( \frac{\Delta}{\lambda} \right)^2 \pi^2 (-6 + 2 \cos(2\phi) - 2 \sin(2\phi) + \sin(4\phi)) \sin^2(2\theta) \right)}{2M \left( - \left( \frac{\Delta}{\lambda} \right)^4 \pi^4 \cos^2(\theta) \sin^2(\phi) (3 \cos(\phi) + \cos(3\phi) + 2 \sin(\phi) - 2 \sin(3\phi))^2 \sin^4(\theta) \right.} \\
&\quad \left. + \frac{1}{4} \left( 1 + 2 \left( \frac{\Delta}{\lambda} \right)^2 \pi^2 (3 + \cos(2\phi) - 2 \sin(2\phi)) \sin^2(\theta) \sin^2(\phi) \right) \right. \\
&\quad \left. \left( 4 + 16 \left( \frac{\Delta}{\lambda} \right)^2 \pi^2 \cos(\phi)^4 \sin^2(\theta) \cos^2(\theta) - \left( \frac{\Delta}{\lambda} \right)^2 \pi^2 (-6 + 2 \cos(2\phi) - 2 \sin(2\phi) + \sin(4\phi)) \sin^2(2\theta) \right) \right).
\end{aligned} \tag{15}$$

These Cramér-Rao bounds are plotted in Figure 3 versus the inter-component spacing  $\left(\frac{\Delta}{\lambda}\right)$ , at a signal-to-noise ratio (SNR) of 0dB, and an incident signal's frequency of 500Hz. These figures show that the Cramér-Rao bounds decrease by orders of magnitude, as the inter-component spacing  $\left(\frac{\Delta}{\lambda}\right)$  increases.

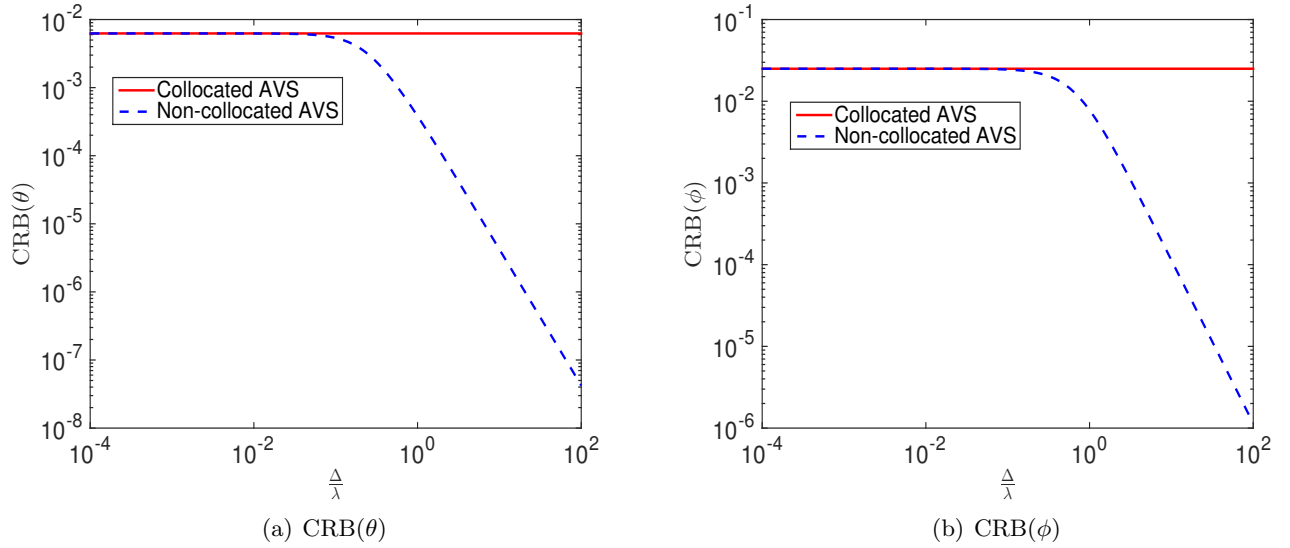


Figure 3: The Cramér-Rao bounds derived in (14)-(15), plotted against the inter-component spacing  $\frac{\Delta}{\lambda}$ , at SNR = 0dB,  $M = 80$ ,  $\theta = \frac{\pi}{6}$ , and  $\phi = \frac{\pi}{4}$ .

## 4 Conclusion

The vector-sensor consists of four component-sensors, which are “traditionally” collocated in a point-like geometry. By spreading these four component-sensors to the four corner of a parallelogram, an extended aperture is realized, thereby improving direction-finding accuracy, without increasing the number of component-sensors. This parallelogram array grid is a special case of the more general grid in [8], which requires slightly more complicated direction-finding formulas than those in this paper. To spread the four component-sensors along a straight line of any orientation in three-dimensional space, please see [12] for closed-form formulas for direction finding.



## References

- [1] A. Nehorai & E. Paldi, "Acoustic vector-sensor array processing," *IEEE Transactions on Signal Processing*, vol. 42, no. 10, pp. 2481-2491, September 1994.
- [2] H. L. Van Trees, *Detection, Estimation and Modulation Theory, Part IV: Optimum Array Processing*, New York, U.S.A.: John Wiley and Sons, 2002.
- [3] J. A. McConnell, "Analysis of a compliantly suspended acoustic velocity sensor," *Journal of the Acoustical Society of America*, vol. 113, no. 3, pp. 1395-1405, March 2003.
- [4] P. K. Tam & K. T. Wong, "Cramér-Rao bounds for direction finding by an acoustic vector-sensor under non-ideal gain-phase responses, non-collocation, or non-orthogonal orientation," *IEEE Sensors Journal*, vol. 9, no. 8, pp. 969-982, August 2009.
- [5] Y. I. Wu, K. T. Wong & S.-K. Lau, "The acoustic vector-sensor's near-field array-manifold," *IEEE Transactions on Signal Processing*, vol. 58, no. 7, pp. 3946-3951, July 2010.
- [6] K. T. Wong, "Acoustic vector-sensor "blind" beamforming & geolocation for FFH-sources," *IEEE Transactions on Aerospace and Electronic Systems*, vol. 46, no. 1, pp. 444-449, January 2010.
- [7] Y. I. Wu & K. T. Wong, "Acoustic near-field source localization by two passive anchor nodes," *IEEE Transactions on Aerospace and Electronic Systems*, vol. 48, no. 1, pp. 159-169, January 2012.
- [8] Y. Song & K. T. Wong, "Azimuth-elevation direction finding using a microphone and three orthogonal velocity sensors as a non-collocated subarray," *Journal of the Acoustical Society of America*, vol. 133, no. 4, pp. 1987-1995, April 2013.
- [9] Y. Song & K. T. Wong, "Acoustic direction finding using a spatially spread tri-axial velocity sensor," *IEEE Transactions on Aerospace and Electronic Systems*, vol. 51, no. 2, pp. 834-842, April 2015.
- [10] Y. Song, K. T. Wong & Y. Li, "Direction finding using a biaxial particle-velocity sensor," *Journal of Sound and Vibration*, vol. 340, pp. 354-367, 2015.
- [11] Y. Song, Y. L. Li & K. T. Wong, "Acoustic direction finding using a pressure sensor and a uniaxial particle velocity sensor," *IEEE Transactions on Aerospace and Electronic Systems*, vol. 51, no. 4, pp. 2560-2569, October 2015.
- [12] Y. Song & K. T. Wong, "Acoustic direction finding using a spatially spread tri-axial velocity sensor," *Proceedings of Meetings on Acoustics*, vol. 23, 2015.